Chemical Science

EDGE ARTICLE

View Article Online
View Journal | View Issue

Cite this: *Chem. Sci.*, 2015, **6**, 472

Annihilation electrogenerated chemiluminescence of mixed metal chelates in solution: modulating emission colour by manipulating the energetics

Emily Kerr,[a] Egan H. Doeven,[a] Gregory J. Barbante,*[a] Conor F. Hogan,*[b] David J. Bower,[b] Paul S. Donnelly,[c] Timothy U. Connell[c] and Paul S. Francis*[a]

Received 3rd September 2014
Accepted 15th October 2014

DOI: 10.1039/c4sc02697g

www.rsc.org/chemicalscience

We demonstrate the mixed annihilation electrogenerated chemiluminescence of tris(2,2′-bipyridine) ruthenium(II) with various cyclometalated iridium(III) chelates. Compared to mixed ECL systems comprising organic luminophores, the absence of T-route pathways enables effective predictions of the observed ECL based on simple estimations of the exergonicity of the reactions leading to excited state production. Moreover, the multiple, closely spaced reductions and oxidations of the metal chelates provide the ability to finely tune the energetics and therefore the observed emission colour. Distinct emissions from multiple luminophores in the same solution are observed in numerous systems. The relative intensity of these emissions and the overall emission colour are dependent on the particular oxidized and reduced species selected by the applied electrochemical potentials. Finally, these studies offer insights into the importance of electronic factors in the question of whether the reduced or oxidized partner becomes excited in annihilation ECL.

Introduction

Electrogenerated chemiluminescence (ECL) is the luminescence arising from electron transfer reactions in which at least one reactant has been electrochemically generated. This phenomenon has not only provided an excellent means for highly sensitive chemical detection,[1–3] but also enabled extensive exploration of exergonic electron-transfer reactions in solution.[4,5] In fact, ECL investigations provided the first experimental verifications of the 'inverted region' of Marcus electron transfer theory,[6,7] where the electron transfer rates of highly exergonic reactions decrease with increasing free energy. Thus, under certain circumstances, the formation of (luminescent) excited states occur at much faster rates than the thermodynamically favoured ground state products.[7]

Central to ECL is the 'annihilation' pathway, in which oxidized and reduced species are formed, usually sequentially, at two different electrode potentials,[1,3] with the subsequent comproportionation of these species generating an emissive excited state. For example, the singlet excited state of an organic luminophore may be generated *via* recombination of its electrogenerated radical anion and cation as in reaction 1–4 (known as the S-route). The oxidized and reduced species can also be generated from different parent compounds, which is referred to as a 'mixed' ECL system.

$$R + e^- \rightarrow R^{\cdot -} \quad (1)$$

$$R - e^- \rightarrow R^{\cdot +} \quad (2)$$

$$R^{\cdot -} + R^{\cdot +} \rightarrow R + {}^1R^* \quad (3)$$

$${}^1R^* \rightarrow {}^1R + h\nu \quad (4)$$

For organic ECL systems, the above excitation process is frequently in competition with generation of the lower-lying triplet excited-state (5). In solution at room temperature, organic triplets are generally non-emissive, but triplet–triplet annihilation can generate the emissive excited state (known as the T-route) (6), even in reactions that lack sufficient energy for direct singlet population (3).[5,8]

$$R^{\cdot -} + R^{\cdot +} \rightarrow R + {}^3R^* \quad (5)$$

$${}^3R^* + {}^3R^* \rightarrow R + {}^1R^* \quad (6)$$

Accordingly, annihilation ECL is somewhat simplified for luminophores exhibiting efficient phosphorescence at room temperature. This includes various transition metal complexes such as tris(2,2′-bipyridine)ruthenium(II) ($Ru(bpy)_3^{2+}$),[9,10] in

[a]*Centre for Chemistry and Biotechnology, School of Life and Environmental Sciences, Faculty of Science, Engineering and Built Environment, Deakin University, Geelong, Victoria 3220, Australia. E-mail: paul.francis@deakin.edu.au; g.barbante@deakin.edu.au*

[b]*Department of Chemistry, La Trobe Institute for Molecular Science, La Trobe University, Melbourne, Victoria 3086, Australia. E-mail: C.Hogan@latrobe.edu.au*

[c]*School of Chemistry and Bio21 Molecular Science and Biotechnology Institute, University of Melbourne, Melbourne 3010, Australia*

which the emission of light from the lowest lying triplet state is facilitated by spin–orbit coupling induced by the heavy-metal ion.

Mixed annihilation systems combining more than one organic compound,[5] or a transition metal chelate with a non-emissive organic compounds,[11–13] have been widely used to study bimolecular electron-transfer reactions and the competitive generation of excited states. Demonstrations of ECL from cyclometalated iridium(III) chelates in recent years,[12–15] with emission maxima spanning the entire visible region, has created new opportunities for multi-colour ECL. Several reports of mixed metal chelate co-reactant ECL systems incorporating ruthenium(II) and iridium(III) complexes have emerged, where excitation is achieved solely by applied oxidative potentials.[16–19] This includes cases in which the emissions were resolved by selective excitation at different potentials.[17–19] Similarly, the co-reactant ECL of $Ru(bpy)_3^{2+}$ and peroxydisulfate has recently been used in conjunction with luminol ECL detection in a potential-resolved immunoassay of two different antigens at a cell surface.[20]

Ruthenium(II) and iridium(III) chelates have also been extensively utilized in light-emitting devices,[3,21] and several research groups have combined an electrochemiluminescent $Ru(bpy)_3^{2+}$ derivative with an electroluminescent material for bias- or potential-controlled switching between emission colours.[22] The use of multiple transition metal chelates in this context offers several major advantages, as demonstrated by Su *et al.*,[23] who combined a blue-green and red emitting iridium(III) complex in a solid-state electrochemical cell to generate white electroluminescence, and Moon *et al.*,[24] who recently created emissive plastic displays based on the mixed annihilation ECL of $Ru(bpy)_3^{2+}$ and $Ir(df\text{-}ppy)_2(bpy)^+$ in block-copolymer-based ion-gels. This approach enabled Moon *et al.* to set the emission colour from orange-red to green, based on the mole ratio of the incorporated complexes.[24]

Despite these impressive advances towards multiplexed ECL detection systems and colour-tuneable light-emitting technologies, annihilation ECL from mixed transition metal-chelate systems in simple solution is yet to be explored. This is surprising, as the fundamental understanding gained from such studies may underpin new developments in these areas. One basic mechanistic question that has remained unanswered in relation to annihilation ECL is whether the reduced or oxidized partner becomes excited following the comproportionation reaction. In the case of ruthenium complexes, formation of an excited state from the reduced parent requires a metal-to-metal electron transfer, whereas formation of an excited state from the oxidized species involves a ligand-to-ligand electron transfer. This suggests that the latter route ought to predominate due to more a favourable electronic factor. By exploring mixed ECL systems where the components have differing localizations of electron density associated with their frontier orbitals, we hope to gain insight into the importance of electronic factors in annihilation ECL.

Utilizing an electrochemical cell coupled with a CCD spectrometer for instantaneous collection of emission spectra, we have examined the multi-colour emissions from a series of mixed annihilation ECL systems containing $Ru(bpy)_3^{2+}$ and various cyclometalated iridium(III) chelates exhibiting green or blue luminescence, to understand and control the relative emission intensities of these novel ECL systems.

Experimental section

Chemicals

Acetonitrile (Ajax Finechem, Australia) was distilled over calcium hydride under grade 5 argon. Solutions were degassed

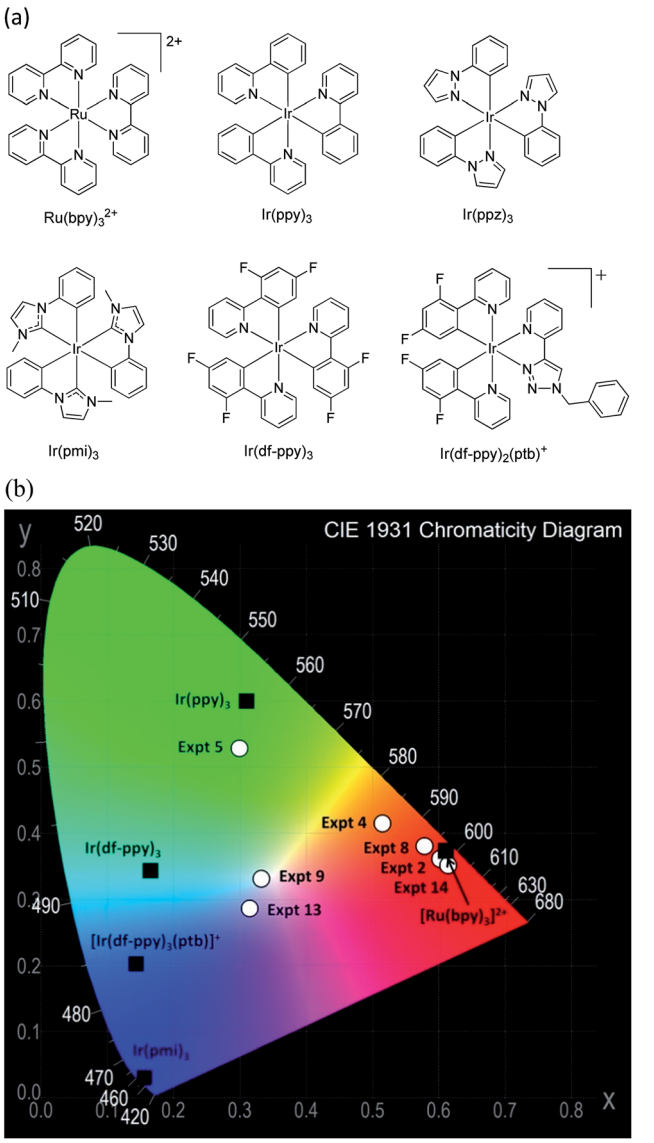

Fig. 1 (a) Ruthenium and iridium complexes used in this study. (b) CIE chromaticity characterization of the photoluminescence of individual complexes (black squares) and the ECL from mixtures of complexes (white circles). The photoluminescence CIE coordinates were obtained using a fluorescence spectrophotometer with integrating sphere and corrected CCD detector.[15] The ECL CIE coordinates were calculated using the mean RGB values[19] for the circular area of the electrode in the photographs shown in subsequent figures. The colour space representation was generated with efg's Computer Lab software.

with argon prior to analysis. The chemical structure and luminescence chromaticity of each ruthenium and iridium complex used in this study is shown in Fig. 1.

Tetrabutylammonium hexafluorophosphate ($TBAPF_6$, 99.5%, electrochemical grade) was purchased from Sigma-Aldrich (Australia). The hexafluorophosphate salt of tris(2,2′-bipyridine-κN1,κN1′)ruthenium(2+) ($[Ru(bpy)_3](PF_6)_2$) was prepared from $Ru(bpy)_3Cl_2 \cdot 6H_2O$ (Strem Chemicals, USA). *fac*-Tris[2-(2-pyridinyl-κN)phenyl-κC]iridium (tris(2-phenylpyridinato-C^2,N)iridium(III); $Ir(ppy)_3$, 99%) and tris[4,6-difluoro-2-(2-pyridyl)phenyl-C^2,N]iridium(III) ($Ir(df\text{-}ppy)_3$) were purchased from Sigma-Aldrich (Australia). Tris[2-(1H-pyrazol-1-yl-κN^2)phenyl-κC]iridium (tris(phenylpyrazole)iridium(III); $Ir(ppz)_3$, >99%) and *fac*-tris(1-phenyl-3-methylimidazolin-2-ylidene-C,C(2′))iridium(III) ($Ir(pmi)_3$, >99%) were purchased from LumTech (Taiwan). Bis[3,5-difluoro-2-(2-pyridinyl-κN)phenyl-κC][2-[1-(phenylmethyl)-1H-1,2,3-triazol-4-yl-κN3]pyridine-κN]-iridium(1+) hexafluorophosphate(1−) ($[Ir(df\text{-}ppy)_2(ptb)](PF_6)$), was synthesized and characterized as previously described.[15]

Experimental procedure

An Autolab PGSTA12 potentiostat was used to perform chronoamperometry and cyclic voltammetry experiments (Metrohm Autolab B.V., Netherlands). A custom-built, light-tight faraday cage encased the electrochemical cell, which consisted of a cylindrical glass cell with a quartz window base and Teflon cover with spill tray. A conventional three-electrode assembly was used throughout, consisting of a glassy carbon (3 mm diameter) working electrode shrouded in Teflon (CH Instruments, Austin, USA), $Ag/AgNO_3$ (0.02 M) reference electrode and platinum wire counter electrode. The glassy carbon working electrode was polished using 0.30 and 0.05 μm alumina on a felt pad with water, rinsed in freshly distilled acetonitrile and dried with nitrogen. The electrode was positioned ~2 mm from the bottom of the cell.

For cyclic voltammetry measurements, the complexes were prepared at equal concentrations in acetonitrile (0.1 M $TBAPF_6$ supporting electrolyte) and the potentials obtained were referenced to the formal potential of the ferrocene/ferrocenium couple (1 mM); measured *in situ* in each case. Prior to analysis, solutions were degassed with grade 5 argon. ECL spectra were obtained using a model QE65pro CCD spectrometer (Ocean Optics). The spectrometer was interfaced with the electrochemical cell through an optic fibre (1 m, 1 mm core diameter) and collimating lens using a custom-built electrochemical cell holder. A HR 4000 Break-Out box was programmed to initiate acquisition at the initiation of the experiment using NOVA software. For annihilation ECL experiments, appropriate concentrations of the complexes (in freshly distilled acetonitrile with 0.1 M $TBAPF_6$ supporting electrolyte) were selected to generate similar emission intensities. Solutions were degassed for 15 min prior to analysis using grade 5 argon. ECL spectra were recorded using a 14 s integration time with Spectra Suite software. NOVA software was employed to configure the potentiostat to apply a 12 s 2-step chronoamperometry pulse to the appropriate applied potentials. Oxidative and reductive potentials for chronoamperometry were determined by cyclic voltammograms prior to each set of ECL experiments.

Results and discussion

Preliminary experiments. $Ru(bpy)_3^{2+}$ with $Ir(ppy)_3$

Cyclic voltammetric scans of a mixture of $Ru(bpy)_3^{2+}$ and $Ir(ppy)_3$ in acetonitrile (containing 0.1 M $TBAPF_6$) show a combination of the characteristic electron-transfer processes of the two metal chelates (Fig. 2b).[12,15,25] This system offers numerous possible reactants for annihilation ECL, which will depend on the applied oxidation and reduction potentials of the alternating electrochemical process. For example, when pulsing 0.1 V beyond the first reduction and oxidation potentials of $Ru(bpy)_3^{2+}$ (as in Expt 1; Fig. 2c), we form not only $Ru(bpy)_3^{+}$ and $Ru(bpy)_3^{3+}$, but also $Ir(ppy)_3^{+}$, for which a series of subsequent reactions to form ground and excited state products can be considered. The free energy (ΔG) of each reaction can be estimated from the separation of the formal potentials of the reactants, and for excited states, from the emission energy (eqn (I) and (II)).[5,26,27]

$$\Delta G_{gs} \approx E^{o}_{A/A-} - E^{o}_{D+/D} \quad (I)$$

$$\Delta G_{es} \approx (E^{o}_{A/A-} - E^{o}_{D+/D}) + E_{es} \quad (II)$$

Where ΔG_{gs} and ΔG_{es} are the free energies of the reactions leading to the ground and excited states respectively; $E^{o}_{A/A-}$ and $E^{o}_{D+/D}$ are the formal potentials of the acceptor and donor species in the annihilation reaction and E_{es} is the energy of the excited state in eV from the emission maximum. These estimations omit the Coulomb repulsion energy required to bring the reactants into the active complex and the vibrational levels of the radiative transition, but as these contributions are small and often opposing, they can (at least to a first approximation) be reasonably neglected.[27,28] In subsequent experiments, we show this approach to be an effective predictor of the observed emissions.

Ground-state products:

$$Ru(bpy)_3^{+} + Ru(bpy)_3^{3+} \rightarrow 2\ Ru(bpy)_3^{2+} \quad (1)$$

$$Ru(bpy)_3^{+} + Ir(ppy)_3^{+} \rightarrow Ru(bpy)_3^{2+} + Ir(ppy)_3 \quad (2)$$

$\Delta G_{gs} = -2.64$ and -2.08 eV, respectively.

One excited-state product:

$$Ru(bpy)_3^{+} + Ru(bpy)_3^{3+} \rightarrow [Ru(bpy)_3^{2+}]^* + Ru(bpy)_3^{2+} \quad (3)$$

$$Ru(bpy)_3^{+} + Ru(bpy)_3^{3+} \rightarrow Ru(bpy)_3^{2+} + [Ru(bpy)_3^{2+}]^* \quad (4)$$

$$Ru(bpy)_3^{+} + Ir(ppy)_3^{+} \rightarrow [Ru(bpy)_3^{2+}]^* + Ir(ppy)_3 \quad (5)$$

$$Ru(bpy)_3^{+} + Ir(ppy)_3^{+} \rightarrow Ru(bpy)_3^{2+} + [Ir(ppy)_3]^* \quad (6)$$

$\Delta G_{es} = -0.63$, -0.63, -0.07, and +0.27 eV, respectively.

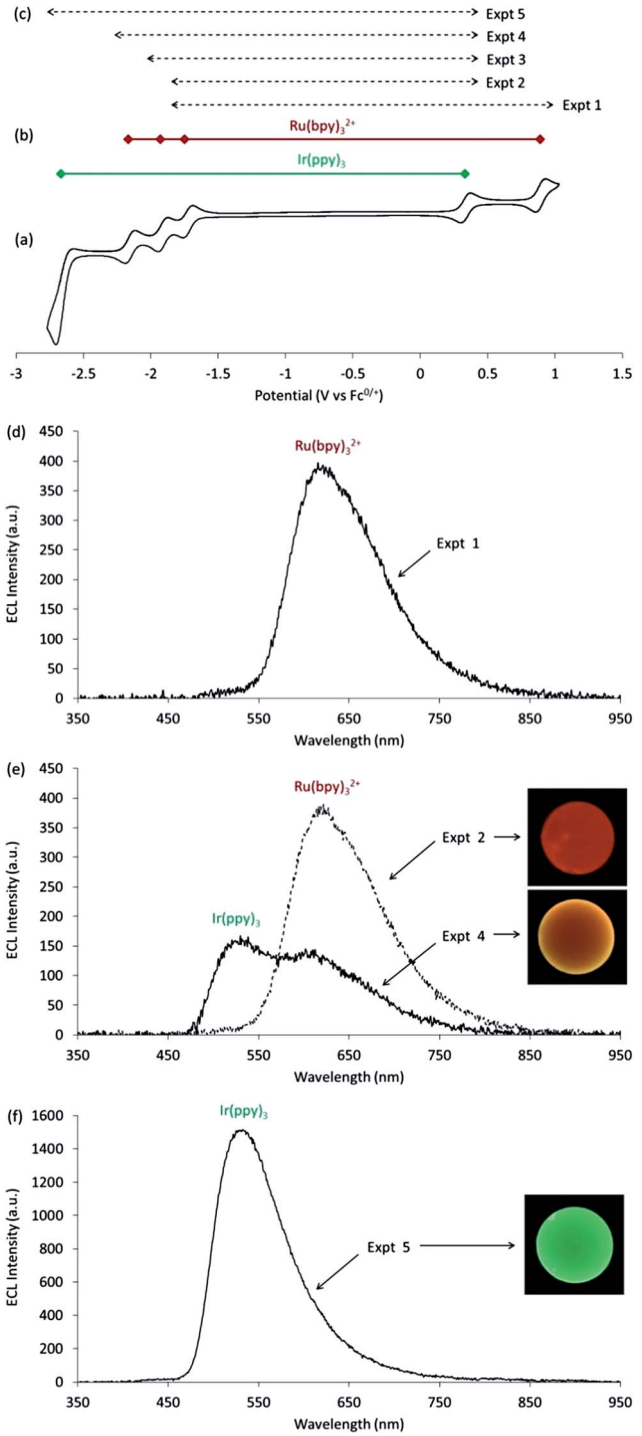

Fig. 2 (a) Cyclic voltammogram of 0.25 mM $Ru(bpy)_3^{2+}$ and 0.25 mM $Ir(ppy)_3$ in acetonitrile containing 0.1 M $TBAPF_6$. (b) Relevant reduction and oxidation potentials of the two metal chelates. (c) Illustration of potentials used in annihilation ECL experiments. (d–f) Spectra and photographs of the ECL at the working electrode of selected annihilation ECL experiments using 0.003 mM $Ru(bpy)_3^{2+}$ and 0.25 mM $Ir(ppy)_3$ in acetonitrile containing 0.1 M $TBAPF_6$.

Two excited-state products:

$$Ru(bpy)_3^{+} + Ru(bpy)_3^{3+} \rightarrow 2\,[Ru(bpy)_3^{2+}]^* \quad (7)$$

$$Ru(bpy)_3^{+} + Ir(ppy)_3^{+} \rightarrow [Ru(bpy)_3^{2+}]^* + [Ir(ppy)_3]^* \quad (8)$$

$\Delta G_{es} = +1.37$, and +2.28 eV, respectively.

Reactions 1 and 2, which form only ground state products, are so exergonic ($\Delta G \ll 0$) that they fall into the Marcus inverted region, and thus are kinetically unfavourable compared to the generation of excited states.[9] On the other hand, reactions 7 and 8, which would form two excited state products, are not thermodynamically feasible ($\Delta G \gg 0$).

The formation of $[Ru(bpy)_3^{2+}]^*$ from the annihilation of $Ru(bpy)_3^{+}$ and $Ru(bpy)_3^{3+}$ is well-known.[1,25] There has been ongoing interest in the subtle question of which of the two parent species forms the excited state,[9] as reactions 3 and 4 are thermodynamically equivalent, and co-reactant 'oxidative-reduction'[29] and 'reductive-oxidation'[30] ECL show that either reactant is capable of forming the excited state.[1] The question of HOMO → HOMO *versus* LUMO → LUMO electron transfer is not easily resolved by experiment, but in the case of the annihilation mechanism, simple orbital overlap arguments suggest that the formation of $[Ru(bpy)_3^{2+}]^*$ from the oxidized parent (involving ligand-to-ligand electron transfer) will be kinetically favoured over formation from the reduced parent (which requires metal-to-metal electron transfer).[9] The investigation of mixed inorganic ECL systems involving iridium complexes offer an interesting means to gain insight into this question because iridium complexes of the type investigated here often have the electron density of their HOMO delocalized over their ligands as well as on the metal. For example, the HOMO of $Ir(ppy)_3$ has been estimated to be less than 50% metal based, on the basis of DFT calculations.[31] Therefore, the HOMO → HOMO electron transfer route ought to be relatively less disfavoured when an iridium complex is the oxidant compared to the case where a ruthenium complex with a purely metal-based HOMO is used.

On the basis of eqn (II), the reaction of $Ru(bpy)_3^{+}$ with $Ir(ppy)_3^{+}$ is sufficiently exergonic to attain $[Ru(bpy)_3^{2+}]^*$ ($\Delta G_{es} < 0$), but not $[Ir(ppy)_3]^*$ ($\Delta G_{es} > 0$). Indeed, only the characteristic orange-red emission of $[Ru(bpy)_3^{2+}]^*$ was observed in Expt 1 (Fig. 2d). We can isolate reaction 5 by applying suitable voltages to generate only $Ru(bpy)_3^{+}$ and $Ir(ppy)_3^{+}$ (Expt 2). Although this isolated mixed system is less exergonic than conventional $Ru(bpy)_3^{2+}$ annihilation ECL, the orange-red emission of $[Ru(bpy)_3^{2+}]^*$ is still observed as predicted (Fig. 2e). The observation of intense orange-red ECL from Expt 2–4 of comparable intensity to Expt 1, shows that the HOMO → HOMO electron transfer route to the excited state is not significantly inhibited in this system.

The reaction of $Ru(bpy)_3^{+}$ with $Ir(ppy)_3^{+}$ does not generate $[Ir(ppy)_3]^*$, but the ruthenium(II) chelate exhibits two additional closely spaced ligand reductions that could be exploited to increase the exergonicity of the $Ir(ppy)_3^{+}$ reduction. Pulsing between the potentials required for the oxidation of $Ir(ppy)_3$ and the second reduction of $Ru(bpy)_3^{2+}$ (Expt 3) did not change the spectral distribution, but pulsing between potentials suitable

for the oxidation of $Ir(ppy)_3$ and the third reduction of $Ru(bpy)_3^{2+}$ (Expt 4) provided sufficient energy to populate the $[Ir(ppy)_3]^*$ state ($\Delta G_{es} < 0$; reaction 10). Experimentally, we observed the combined orange-red ECL of $[Ru(bpy)_3^{2+}]^*$ and green ECL of $[Ir(ppy)_3]^*$ as a yellow emission (Fig. 2e, Expt 4), which can be confidently ascribed to reactions 5 and 10.

$$Ru(bpy)_3 + Ir(ppy)_3^+ \rightarrow Ru(bpy)_3^+ + [Ir(ppy)_3]^* \quad (9)$$

$$Ru(bpy)_3^- + Ir(ppy)_3^+ \rightarrow Ru(bpy)_3 + [Ir(ppy)_3]^* \quad (10)$$

$\Delta G_{es} = +0.09$ eV, and -0.15 eV, respectively.

In the previously explored annihilation-ECL systems containing mixtures of organic molecules,[5] the luminescence was often found to emanate from the lowest lying singlet excited state of one of the emitters, after either direct population or efficient energy transfer. One explanation for the simultaneous ECL from two distinct emitters in Expt 4 could be the large difference in the concentration of the two metal chelates, and thus an insufficient concentration of $Ru(bpy)_3^{2+}$ for significant energy transfer from the higher energy $[Ir(ppy)_3]^*$ emitter. However, there is very little overlap in their respective absorption and emission bands (due in part to the large Stokes shift of their phosphorescent emissions). Furthermore, mixed electrochemiluminophore co-reactant ECL experiments have shown that the emission from $[Ir(ppy)_3]^*$ can occur in the presence of $Ru(bpy)_3^{2+}$ without significant energy transfer.[18,19]

In Expt 1–4, the limiting reactants for annihilation ECL in terms of concentration are the reduced ruthenium complexes. However, when $Ir(ppy)_3$ was also reduced (*e.g.* Expt 5), relatively high concentrations of both $Ir(ppy)_3^+$ and $Ir(ppy)_3^-$ were formed, and the characteristic green emission of $[Ir(ppy)_3]^*$ was dominant (reaction 11 and Fig. 2f).

$$Ir(ppy)_3^- + Ir(ppy)_3^+ \rightarrow [Ir(ppy)_3]^* + Ir(ppy)_3 \quad (11)$$

$\Delta G_{es} = -0.65$ eV.

The mean RGB data from the photographs of the mixed annihilation ECL near the electrode surface were used to calculate the CIE chromaticity. For experiments in which the emission was found to occur from only one metal complex (*e.g.*, $[Ru(bpy)_3^{2+}]^*$ in Expt 2, or $[Ir(ppy)_3]^*$ in Expt 5), the CIE coordinates were in reasonable agreement with those obtained from photoluminescence experiments using a spectrometer with integrating sphere and corrected CCD detector (Fig. 1b), despite difference in the responses of the digital camera and CCD detector over the visible region. For experiments that led to more than one emitting species (*e.g.*, $[Ru(bpy)_3^{2+}]^*$ and $[Ir(ppy)_3]^*$ in Expt 4), intermediate CIE coordinates were obtained (Fig. 1b).

Mixing emissive and non-emissive metal chelate species. $Ru(bpy)_3^{2+}$ with $Ir(ppz)_3$

The above findings suggest that annihilation ECL should also be possible using a mixture of $Ru(bpy)_3^{2+}$ and a non-emissive iridium complex with similar oxidation potential to $Ir(ppy)_3$, without needing to generate the oxidized $Ru(bpy)_3^{3+}$ species. For this experiment, we selected $Ir(ppz)_3$, which has a photoluminescence quantum yield below 0.01 at room temperature, due to efficient population of a non-emissive metal centred (^{3}MC) excited state.[32] The reduction potential of $Ir(ppz)_3$ is outside the potential window of the acetonitrile solvent, but its oxidation potential (0.38 V *vs.* $Fc^{0/+}$) is marginally higher than that of $Ir(ppy)_3$ (0.33 V *vs.* $Fc^{0/+}$), ensuring $\Delta G < 0$ for the generation of $[Ru(bpy)_3]^{2+}$* (reaction 12). The application of alternating potentials sufficient to create these precursors (Expt 6, Fig. 3) resulted in the characteristic emission from $[Ru(bpy)_3]^{2+}$* (Fig. 3d).

$$Ru(bpy)_3^+ + Ir(ppz)_3^+ \rightarrow [Ru(bpy)_3^{2+}]^* + Ir(ppz)_3 \quad (12)$$

$\Delta G_{es} = -0.12$ eV.

Population of the $[Ru(bpy)_3^{2+}]^*$ excited state *via* an energy transfer pathway can effectively be ruled out due to the low luminescent quantum yield of $Ir(ppz)_3$. Therefore the intense orange-red emission observed in this system is due to efficient HOMO → HOMO electron transfer in reaction 12.

An energy insufficient metal chelate system. $Ru(bpy)_3^{2+}$ with $Ir(pmi)_3$

Although the reactions of $Ru(bpy)_3^+$ with $Ir(ppy)_3^+$ (Expt 2) or $Ir(ppz)_3^+$ (Expt 6) are less exergonic than that of $Ru(bpy)_3^+$ with

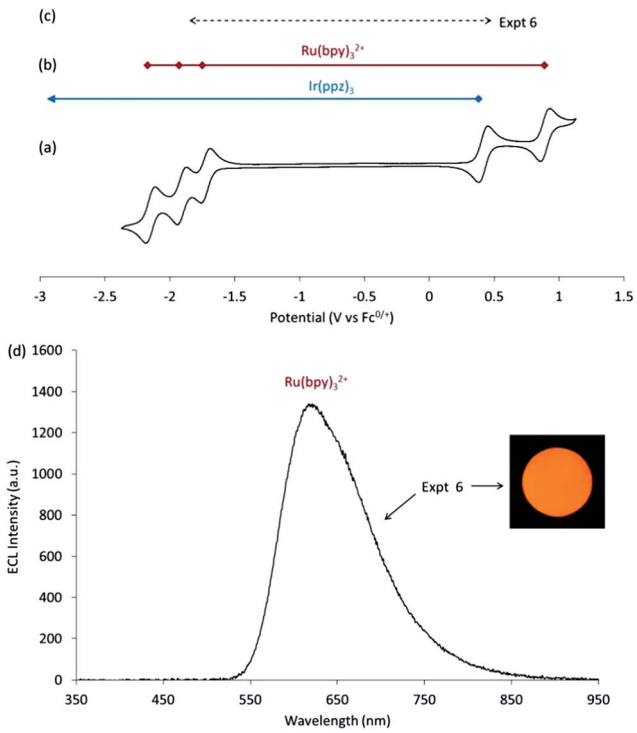

Fig. 3 (a) Cyclic voltammogram of 0.5 mM $Ru(bpy)_3^{2+}$ and 0.5 mM $Ir(ppz)_3$ in acetonitrile containing 0.1 M $TBAPF_6$. (b) Relevant reduction and oxidation potentials of the two metal chelates. (c) Illustration of potentials used in annihilation ECL experiments. (d) Spectrum and photograph of the ECL at the working electrode of annihilation ECL Expt 6, using 0.01 mM $Ru(bpy)_3^{2+}$ and 0.5 mM $Ir(ppz)_3$ in acetonitrile containing 0.1 M $TBAPF_6$.

$Ru(bpy)_3^{3+}$, they can each directly populate the $[Ru(bpy)_3]^{2+}$* excited state. The oxidation potential of $Ir(pmi)_3$ (0.22 V *vs.* $Fc^{0/+}$), however, is lower than that of $Ir(ppy)_3$, and although both species are photoluminescent, the generation of $[Ru(bpy)_3]^{2+}$* or $[Ir(pmi)_3]$* from the reaction of $Ru(bpy)_3^{+}$ with $Ir(pmi)_3^{+}$ (Expt 7; data not shown) is not feasible (reactions 13 and 14).

$$Ru(bpy)_3^{+} + Ir(pmi)_3^{+} \rightarrow [Ru(bpy)_3^{2+}]^* + Ir(pmi)_3 \quad (13)$$

$$Ru(bpy)_3^{+} + Ir(pmi)_3^{+} \rightarrow Ru(bpy)_3^{2+} + [Ir(pmi)_3]^* \quad (14)$$

$\Delta G_{es} = +0.04$, and +1.26 eV, respectively.

As predicted, no significant ECL was observed from this experiment. Unlike many 'energy-insufficient' systems comprising organic molecules,[5] the initial population of lower energy excited states, followed by up-conversion to generate the emissive excited state, is not possible in these mixed metal-chelate systems where the emission occurs from short-lived triplets.[9,10,33]

Manipulating emission in mixed metal chelate ECL systems

(i) Dominant emission determined by reduced species. $Ru(bpy)_3^{2+}$ with $Ir(df\text{-}ppy)_3$. The oxidation potential of $Ir(df\text{-}ppy)_3$ is 0.21 V less positive than $Ru(bpy)_3^{2+}$, and the reduction potential of $Ir(df\text{-}ppy)_3$ is 0.36 V more negative than the third reduction of $Ru(bpy)_3^{2+}$. Under these experimental conditions, pulsing 0.1 V beyond the first reduction of $Ru(bpy)_3^{2+}$ in conjunction with one or both oxidized metal chelates (*e.g.* Expt 8 or 10) produced a strong orange-red emission from $[Ru(bpy)_3^{2+}]$* and a weak blue emission from $[Ir(df\text{-}ppy)_3]$*. In contrast, pulsing beyond the reduction of $Ir(df\text{-}ppy)_3$ in conjunction with one or both oxidized metal chelates (*e.g.* Expt 9 or 11) generated a large emission from both $[Ir(df\text{-}ppy)_3]$* and $[Ru(bpy)_3^{2+}]$*. For example, the ECL spectra for Expt 8 and 9 are shown in Fig. 4d. Once again the unexpectedly high efficiency of the HOMO → HOMO electron transfer route to the excited state is evident in the intense orange-red ECL emission observed in Expt 8 and 9.

In both Expt 8 and 9, $[Ru(bpy)_3^{2+}]$* is formed by the oxidation of $Ru(bpy)_3^{+}$ (reaction 15), but in Expt 9 this immediate precursor is not initially the dominant form of the ruthenium chelate at the electrode. In Expt 8, small amounts of $[Ir(df\text{-}ppy)_3]$* are formed from the reduction of $Ir(df\text{-}ppy)_3^{+}$ (reaction 16, $\Delta G_{es} \approx 0$), but in Expt 9 this emitter may be formed from reactions 17 and 18. At these metal chelate concentrations, $[Ru(bpy)_3^{2+}]$* dominates in Expt 8, and the emission from $[Ir(df\text{-}ppy)_3]$* is greater in Expt 9 (Fig. 4d). Similar reasoning can be presented for Expt 10 and 11. The dominant emission colour in this system is therefore largely determined by the applied reduction potential of the electrochemical process, if the applied oxidation potential is at least sufficient to achieve the first metal-chelate oxidation.

$$Ru(bpy)_3^{+} + Ir(df\text{-}ppy)_3^{+} \rightarrow [Ru(bpy)_3^{2+}]^* + Ir(df\text{-}ppy)_3 \quad (15)$$

$$Ru(bpy)_3^{+} + Ir(df\text{-}ppy)_3^{+} \rightarrow Ru(bpy)_3^{2+} + [Ir(df\text{-}ppy)_3]^* \quad (16)$$

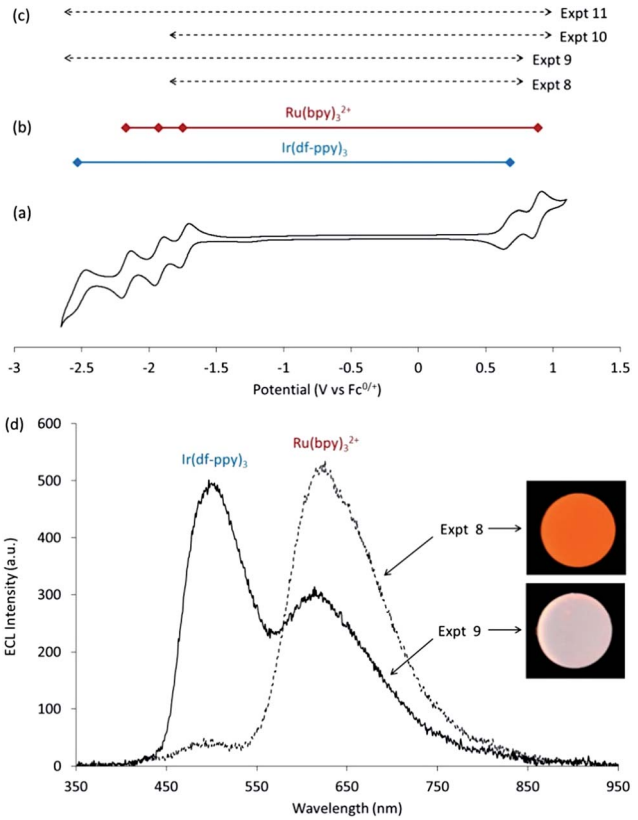

Fig. 4 (a) Cyclic voltammogram of 0.25 mM $Ru(bpy)_3^{2+}$ and 0.25 mM $Ir(df\text{-}ppy)_3$ in acetonitrile containing 0.1 M $TBAPF_6$. (b) Relevant reduction and oxidation potentials of the two metal chelates. (c) Illustration of potentials used in annihilation ECL experiments. (d) Spectra and photographs of the ECL at the working electrode of selected annihilation ECL experiments using 0.01 mM $Ru(bpy)_3^{2+}$ and 0.25 mM $Ir(df\text{-}ppy)_3$ in acetonitrile containing 0.1 M $TBAPF_6$.

$$Ru(bpy)_3^{-} + Ir(df\text{-}ppy)_3^{+} \rightarrow Ru(bpy)_3^{2+} + [Ir(df\text{-}ppy)_3]^* \quad (17)$$

$$Ir(df\text{-}ppy)_3^{-} + Ir(df\text{-}ppy)_3^{+} \rightarrow Ir(df\text{-}ppy)_3 + [Ir(df\text{-}ppy)_3]^* \quad (18)$$

$\Delta G_{es} = -0.63$, +0.07, −0.35, and −0.71 eV, respectively.

(ii) Dominant emitter determined by oxidized species. $Ru(bpy)_3^{2+}$ with $Ir(df\text{-}ppy)_2(ptb)^{+}$. The first reduction and oxidation potentials of $Ru(bpy)_3^{2+}$ lie inside those of $Ir(df\text{-}ppy)_2(ptb)^{+}$ (Fig. 5). This enables the selective generation of $[Ru(bpy)_3^{2+}]$* without any electrochemical interaction between $Ir(df\text{-}ppy)_2(ptb)^{+}$ and electrode (Expt 12). The ECL intensity in this case, however, was weak, because of the low concentration of $Ru(bpy)_3^{2+}$ (the precursor to both the oxidized and reduced reactants in Expt 12) in this group of experiments. Nevertheless, extending the applied voltages to include the oxidation (Expt 13) or reduction (Expt 14) of $Ir(df\text{-}ppy)_2(ptb)^{+}$ resulted in ECL from both $[Ru(bpy)_3^{2+}]$* and $[Ir(df\text{-}ppy)_2(ptb)^{+}]$*, but at considerably different ratios (Fig. 5d). All mixed annihilation reactions in these experiments are sufficiently exergonic to form either emitter (reactions 19–22).

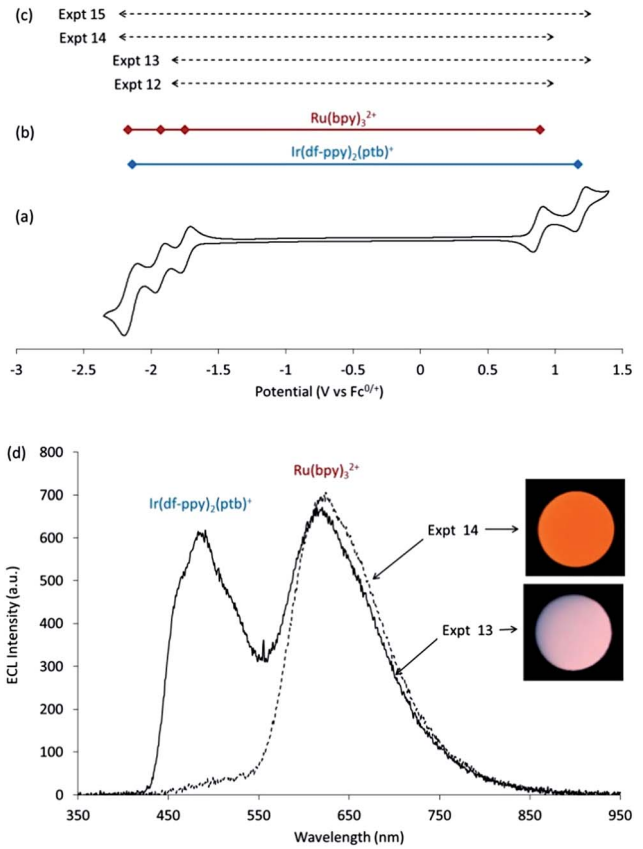

Fig. 5 (a) Cyclic voltammogram of 0.5 mM $Ru(bpy)_3^{2+}$ and 0.5 mM $Ir(df\text{-}ppy)_2(ptb)^+$ in acetonitrile containing 0.1 M $TBAPF_6$. (b) Relevant reduction and oxidation potentials of the two metal chelates. (c) Illustration of potentials used in annihilation ECL experiments. (d) Spectra and photographs of the ECL at the working electrode of selected annihilation ECL experiments using 0.004 mM $Ru(bpy)_3^{2+}$ and 0.4 mM $Ir(df\text{-}ppy)_2(ptb)^+$ in acetonitrile containing 0.1 M $TBAPF_6$.

$$Ru(bpy)_3^{+} + Ir(df\text{-}ppy)_2(ptb)^{2+} \rightarrow Ru(bpy)_3^{2+} + [Ir(df\text{-}ppy)_2(ptb)^{+}]^* \quad (19)$$

$$Ru(bpy)_3^{+} + Ir(df\text{-}ppy)_2(ptb)^{2+} \rightarrow [Ru(bpy)_3^{2+}]^* + Ir(df\text{-}ppy)_2(ptb)^{+} \quad (20)$$

$$Ru(bpy)_3^{3+} + Ir(df\text{-}ppy)_2(ptb) \rightarrow Ru(bpy)_3^{2+} + [Ir(df\text{-}ppy)_2(ptb)^{+}]^* \quad (21)$$

$$Ru(bpy)_3^{3+} + Ir(df\text{-}ppy)_2(ptb) \rightarrow [Ru(bpy)_3^{2+}]^* + Ir(df\text{-}ppy)_2(ptb)^{+} \quad (22)$$

$\Delta G_{es} = -0.19$, -0.91, -0.30, and -1.02 eV, respectively.

Notably in Expt 14, it is the iridium excited state that is populated by electron transfer from the HOMO of the ruthenium complex to the HOMO of the iridium complex, though with seemingly lower efficiency than the previously cases where the iridium HOMO is the donor.

Further extending the applied potential range to include both the reduction and oxidation of $Ir(df\text{-}ppy)_2(ptb)^+$ (Expt 15) resulted in a similar ECL spectral distribution to that of Expt 13. Therefore, in contrast to the above system, the dominant emission in this case is largely determined by the applied oxidation potential, so long as the other applied potential was at least beyond the first reduction. In Expt 13 and Expt 9, the combined emissions spanned the entire visible region, resulting in near-white luminescence (Fig. 1b, 4d, and 5d).

Conclusions

The mixed annihilation ECL of metal chelates provides an alternative approach to multi-colour ECL, in which the relative intensity of the emissions from multiple luminophores (and hence overall emission colour) can be controlled initially by selection of the electrochemical and spectroscopic properties of the complexes, and then the applied electrochemical potentials. The absence of the up-conversion processes often encountered in 'energy insufficient' organic mixed systems simplifies predictions of excited state generation. Furthermore, the numerous closely spaced reductions and oxidations of the mixed systems enable fine tuning of the reaction energy and hence control of the resulting ECL emission colour. Apart from the relevance of these studies to research into voltage controllable light emitting devices, the observation of efficient HOMO → HOMO electron transfer pathways in these mixed systems offers interesting insights into the somewhat intractable question of whether the reduced or oxidized partner becomes the excited state in classic annihilation ECL experiments. In the case of ruthenium complexes where the HOMO is almost exclusively metal-based, it is generally believed that electron transfer between LUMOs is strongly preferred due to more favourable orbital overlap compared with the alternative HOMO → HOMO transfer where the reduced partner becomes excited. Our results tend to support this analysis, because the delocalized nature of the HOMO in the case of the iridium complexes studied here renders this electronic factor less unfavourable, resulting in higher than expected ECL intensities in cases where $Ru(bpy)_3^+$ forms an excited state by loss of an electron from its HOMO.

Acknowledgements

This research was funded by the Australian Research Council (FT100100646).

Notes and references

1 M. M. Richter, *Chem. Rev.*, 2004, **104**, 3003–3036; W. Miao, *Chem. Rev.*, 2008, **108**, 2506–2553.
2 N. D. Danielson, in *Electrogenerated Chemiluminescence*, ed. A. J. Bard, Marcel Dekker, New York, 2004, pp. 397–444; B. A. Gorman, P. S. Francis and N. W. Barnett, *Analyst*, 2006, **131**, 616–639; R. J. Forster, P. Bertoncello and T. E. Keyes, *Annu. Rev. Anal. Chem.*, 2009, **2**, 359–385; T. Joshi, G. J. Barbante, P. S. Francis, C. F. Hogan, A. M. Bond, G. Gasser and L. Spiccia, *Inorg. Chem.*, 2012, **51**, 3302–3315; X. Zhou, D. Zhu, Y. Liao, W. Liu, H. Liu, Z. Ma and D. Xing, *Nat. Protoc.*, 2014, **9**, 1146–1159.

3 L. Hu and G. Xu, *Chem. Soc. Rev.*, 2010, **39**, 3275–3304.
4 A. Kapturkiewicz, in *Electrogenerated Chemiluminescence*, ed. A. J. Bard, Marcel Dekker, New York, 2004, pp. 163–211.
5 S. P. Forry and R. M. Wightman, in *Electrogenerated Chemiluminescence*, ed. A. J. Bard, Marcel Dekker, New York, 2004, pp. 273–299.
6 R. A. Marcus, *J. Chem. Phys.*, 1956, **24**, 966–978; R. A. Marcus, *J. Chem. Phys.*, 1965, **43**, 2654–2657; Y. Zu, F.-R. F. Fan and A. J. Bard, *J. Phys. Chem. B*, 1999, **103**, 6272–6276.
7 A. Kapturkiewicz, *Adv. Electrochem. Sci. Eng.*, 1997, **5**, 1–60.
8 D. J. Freed and L. R. Faulkner, *J. Am. Chem. Soc.*, 1971, **93**, 2097–2102; E. M. Gross, J. D. Anderson, A. F. Slaterbeck, S. Thayumanavan, S. Barlow, Y. Zhang, S. R. Marder, H. K. Hall, M. F. Nabor, J.-F. Wang, E. A. Mash, N. R. Armstrong and R. M. Wightman, *J. Am. Chem. Soc.*, 2000, **122**, 4972–4979.
9 A. Juris, V. Balzani, F. Barigelletti, S. Campagna, P. Belser and A. Von Zelewsky, *Coord. Chem. Rev.*, 1988, **84**, 85–277.
10 S. Campagna, F. Puntoriero, F. Nastasi, G. Bergamini and V. Balzani, *Top. Curr. Chem.*, 2007, **280**, 117–214.
11 A. Kapturkiewicz, P. Szrebowaty, G. Angulo and G. Grampp, *J. Phys. Chem. A*, 2002, **106**, 1678–1685; A. Kapturkiewicz and P. Szrebowaty, *J. Chem. Soc., Dalton Trans.*, 2002, 3219–3225; A. Kapturkiewicz, T.-M. Chen, I. R. Laskar and J. Nowacki, *Electrochem. Commun.*, 2004, **6**, 827–831.
12 A. Kapturkiewicz and G. Angulo, *Dalton Trans.*, 2003, 3907–3913.
13 A. Kapturkiewicz, J. Nowacki and P. Borowicz, *Electrochim. Acta*, 2005, **50**, 3395–3400.
14 A. Vogler and H. Kunkely, *ACS Symp. Ser.*, 1987, **333**, 155–168; S. Zanarini, M. Felici, G. Valenti, M. Marcaccio, L. Prodi, S. Bonacchi, P. Contreras-Carballada, R. M. Williams, M. C. Feiters, R. J. M. Nolte, L. De Cola and F. Paolucci, *Chem.–Eur. J.*, 2011, **17**, 4640–4647.
15 G. J. Barbante, E. H. Doeven, E. Kerr, T. U. Connell, P. S. Donnelly, J. M. White, T. Lópes, S. Laird, C. F. Hogan, D. J. D. Wilson, P. J. Barnard and P. S. Francis, *Chem.–Eur. J.*, 2014, **20**, 3322–3332.
16 D. Bruce and M. M. Richter, *Anal. Chem.*, 2002, **74**, 1340–1342; B. D. Muegge and M. M. Richter, *Anal. Chem.*, 2004, **76**, 73–77.
17 E. H. Doeven, E. M. Zammit, G. J. Barbante, C. F. Hogan, N. W. Barnett and P. S. Francis, *Angew. Chem., Int. Ed.*, 2012, **51**, 4354–4357.
18 E. H. Doeven, E. M. Zammit, G. J. Barbante, P. S. Francis, N. W. Barnett and C. F. Hogan, *Chem. Sci.*, 2013, **4**, 977–982.
19 E. H. Doeven, G. J. Barbante, E. Kerr, C. F. Hogan, J. A. Endler and P. S. Francis, *Anal. Chem.*, 2014, **86**, 2727–2732.
20 F. Han, H. Jiang, D. Fang and D. Jiang, *Anal. Chem.*, 2014, **86**, 6896–6902.
21 C. H. Lyons, E. D. Abbas, J. K. Lee and M. F. Rubner, *J. Am. Chem. Soc.*, 1998, **120**, 12100–12107; E. S. Handy, A. J. Pal and M. F. Rubner, *J. Am. Chem. Soc.*, 1999, **121**, 3525–3528; F. G. Gao and A. J. Bard, *J. Am. Chem. Soc.*, 2000, **122**, 7426–7427; M. K. Nazeeruddin, R. Humphry-Baker, D. Berner, S. Rivier, L. Zuppiroli and M. Graetzel, *J. Am. Chem. Soc.*, 2003, **125**, 8790–8797; H. J. Bolink, L. Cappelli, E. Coronado, M. Grätzel, E. Orti, R. D. Costa, P. M. Viruela and M. K. Nazeeruddin, *J. Am. Chem. Soc.*, 2006, **128**, 14786–14787; L. He, L. Duan, J. Qiao, R. Wang, P. Wei, L. Wang and Y. Qiu, *Adv. Funct. Mater.*, 2008, **18**, 2123–2131; M. Mydlak, C. Bizzarri, D. Hartmann, W. Sarfert, G. Schmid and L. De Cola, *Adv. Funct. Mater.*, 2010, **20**, 1812–1820.
22 S. Welter, K. Brunner, J. W. Hofstraat and L. De Cola, *Nature*, 2003, **421**, 54–57; C. Zhen, Y. Chuai, C. Lao, L. Huang, D. Zou, D. N. Lee and B. H. Kim, *Appl. Phys. Lett.*, 2005, **87**, 093508; F. Wang, P. Wang, X. Fan, X. Dang, C. Zhen, D. Zou, E. H. Kim, D. N. Lee and B. H. Kim, *Appl. Phys. Lett.*, 2006, **89**, 183519.
23 H.-C. Su, H.-F. Chen, F.-C. Fang, C.-C. Liu, C.-C. Wu, K.-T. Wong, Y.-H. Liu and S.-M. Peng, *J. Am. Chem. Soc.*, 2008, **130**, 3413–3419.
24 H. C. Moon, T. P. Lodge and C. D. Frisbie, *J. Am. Chem. Soc.*, 2014, **136**, 3705–3712.
25 N. E. Tokel and A. J. Bard, *J. Am. Chem. Soc.*, 1972, **94**, 2862–2863.
26 A. Vogler, H. Kunkely and S. Schäffl, *ACS Symp. Ser.*, 1986, **307**, 120–134.
27 A. Kapturkiewicz, *Chem. Phys. Lett.*, 1995, **236**, 389–394.
28 G. J. Barbante, C. F. Hogan, D. J. D. Wilson, N. A. Lewcenko, F. M. Pfeffer, N. W. Barnett and P. S. Francis, *Analyst*, 2011, **136**, 1329–1338.
29 M.-M. Chang, T. Saji and A. J. Bard, *J. Am. Chem. Soc.*, 1977, **99**, 5399–5403.
30 H. S. White and A. J. Bard, *J. Am. Chem. Soc.*, 1982, **104**, 6891–6895.
31 R. V. Kiran, C. F. Hogan, B. D. James and D. J. D. Wilson, *Eur. J. Inorg. Chem.*, 2011, 4816–4825.
32 T. Sajoto, P. I. Djurovich, A. B. Tamayo, J. Oxgaard, W. A. Goddard and M. E. Thompson, *J. Am. Chem. Soc.*, 2009, **131**, 9813–9822.
33 L. Flamigni, A. Barbieri, C. Sabatini, B. Ventura and F. Barigelletti, *Top. Curr. Chem.*, 2007, **281**, 143–203.